Influence of Transitions between SI and HCCI Combustion on Driving Cycle Fuel Consumption

Sandro Nüesch[1], Erik Hellström[1], Li Jiang[2] and Anna Stefanopoulou[1]

Abstract— A model for a vehicle equipped with a multimode combustion engine is formulated and calibrated to experiments. A study is performed for the FTP-75 driving cycle about the influence of the mode switch strategy on the engine operation and fuel consumption, using simulation results and driving cycle measurements. It is found that the fuel penalty for mode transitions cancels a significant part of the theoretical benefits of advanced combustion modes. A smoothing strategy, where a mode switch is delayed, is introduced and it is shown that, by computing the optimal wait time, the negative influence of mode transitions on the overall efficiency can be reduced.

I. INTRODUCTION

Improvements in fuel consumption and reductions in emissions are essential goals in research about internal combustion engines. One way towards achieving those goals is the development of advanced engine and combustion technologies, such as homogeneous charge compression ignition (HCCI). Combustion variability and high pressure-rise rates currently constrain the range of naturally aspirated (NA) HCCI operation between low and medium loads. Compared to the full region of a conventional SI engine the NA HCCI regime is limited. Nevertheless, part-load regimes are frequently visited during typical driving and are regimes where a traditional SI engine is relatively inefficient, mainly due to the need for throttling.

An engine to driving cycle model was used in [5] to predict the theoretical improvements in fuel consumption with an HCCI/SI engine on several driving cycles. The combustion mode switches were assumed instantaneous and without fuel penalties. However, based on previous work on combustion mode switches and strategies to control them (see e.g. [7], [12] and [1]) it is expected that a switch will incur a fuel penalty and require a number of engine cycles to complete. The goal of this work is therefore to analyze the influence of those penalties on a driving cycle. Even though the gain of using HCCI would most likely be higher for a highway driving cycle, the one given by the federal test procedure FTP-75 was analyzed since the effect of mode switching is more significant due to the dynamic driving behavior.

To be able to make predictions for a variation of transition settings a dynamic vehicle model is developed and param-

[1]S. Nüesch, E. Hellström and A. Stefanopoulou are with the Department of Mechanical Engineering in the University of Michigan, Ann Arbor, MI 48109, USA
[2]L. Jiang is with Robert Bosch LLC, Farmington Hills, MI 48331, USA

eterized for the Cadillac CTS. A clutch model with slip is implemented for the modeling of start, stop and gear shifts.

The paper is organized as follows: First the models of engine, driver and vehicle are explained and validated. Then the transitions between SI and HCCI, the influence of their fuel penalty and the delay of the switch are analyzed.

II. ENGINE MODEL

A. Engine Maps and Operating Regions

Maps interpolating steady-state experiments are used to compute engine torque T_e and fuel consumption $\dot{m}_f$ from acceleration pedal position u_a and engine speed ω_e. Therefore the simulation is not able to reproduce transient phenomena on engine level, which are faster than the drive cycle dynamics, e.g. manifold filling dynamics, thermal inertia effects etc., hence associated penalties in fuel consumption are not accounted for. In general those penalties can be significant (see [9] and [3]). The aim here is to study the influence of the combustion mode switches and hence only the switch transients are considered.

The map of the original engine of the baseline vehicle, a 3.6L V6, was used for validation of the model with real world driving measurements. This engine has been downsized and turbocharged to a 2.0L I4 in order to improve fuel economy, which is a popular trend in industry. To achieve an additional efficiency gain this engine is modified (e.g. higher compression ratio) to a multi mode combustion engine, able to run lean HCCI in a small regime which is generally characterized by lower break specific fuel consumption (BSFC) compared to SI mode and ultra low NO_x emissions. Experiments have been performed to identify the feasible regime for HCCI combustion for the particular engine and to indicate the fuel efficiency improvement of lean HCCI over SI combustion mode. Therefore the BSFC map of the SI-only 2.0L I4 is used and modified in this study by including the HCCI regime. For very low loads the fuel consumption of SI and HCCI was extrapolated. Restrictive assumptions have been used in the sense that the difference in BSFC between SI and HCCI might be rather larger in reality.

The engine torque $T_e(u_a, \omega_e)$ is mapped over engine speed ω_e and acceleration pedal position u_a, as input for the SI BSFC map. If the HCCI mode is enabled, it is first verified that T_e and ω_e lie inside the feasible boundaries for HCCI combustion. If so, the BSFC of the HCCI map is used. The currently beneficial operating mode is described by R.

Fig. 1 represents the combined BSFC maps of the 2.0L I4 for SI and HCCI combustion. The red dashed regime corresponds to $R = HCCI$. In average HCCI results in a

13.4% lower BSFC than SI, but the benefit can go up to 20% for low loads.

Note that advanced combustion strategies, such as multi injection and multi ignition (MIMI) [11] or boosted HCCI can expand the NA basic HCCI region shown in this paper.
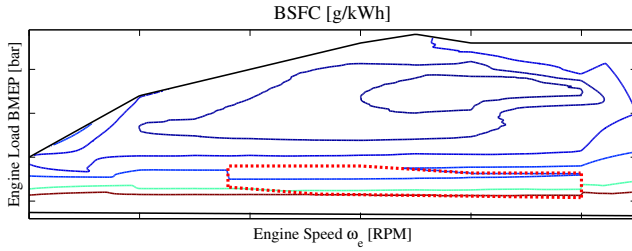

Fig. 1. 2.0L SI BSFC map (black) combined with the operating regime of lean HCCI with negligible NO_x (red)

B. Combustion Modes

The combustion modes are defined as state M. Besides the two main modes SI and HCCI two additional intermediate modes are introduced: The wait mode w is used to delay a mode switch from SI to HCCI. The number of cycles since the last mode switch are denoted by state n. If the input, the beneficial region R, switches from SI to HCCI, the combustion mode M remains w until either the currently beneficial region $R(k)$ switches back to SI or a specified number of engine cycles, denoted as parameter n_w, has been reached. In the first case during the next time step the mode switches back to SI mode, in the second case the transition mode *trans* is started to switch forward to HCCI.

$$M(k+1) = \begin{cases} w & n(k) < n_w \wedge R(k) = \text{HCCI} \\ SI & n(k) < n_w \wedge R(k) = \text{SI} \\ trans & n(k) \geq n_w \end{cases} \quad (1)$$

The mode $M = trans$ is the state of the engine responsible for changing the combustion properties in order to enable a switch to a new mode. Experimental results of combustion mode transitions are shown in [10] and [13]. In order to switch to HCCI, the engine has to operate unthrottled SI and the valves need to be placed in positions feasible for HCCI. Due to the larger amount of air the fuel needs to be increased in order to keep stoichiometric conditions. In this model a constant penalty factor d is assumed and multiplied with the SI fuel consumption during mode transitions. Parameter n_t represents the number of cycles, that are required to prepare the engine for HCCI mode. Studies, connected to [1], performed by a co-investigator under the same project have suggested $n_w = 1$ cycle as minimum to prepare the mode switch, $n_t = 5$ cycles and $d = 1.25$ as preliminary assumptions. After n_t cycles the engine switches to the currently beneficial region $R(k)$ during the next time step $k+1$,

$$M(k+1) = \begin{cases} trans & n(k) < n_t \\ R(k) & n(k) \geq n_t. \end{cases} \quad (2)$$

During switches from HCCI to SI the wait mode w is not visited but the transition still requires time. Therefore if $M = HCCI$ the combustion mode is switched into transition mode *trans* again as soon as $R \neq HCCI$.

$$M(k+1) = \begin{cases} HCCI & R(k) = HCCI \\ trans & R(k) = SI. \end{cases} \quad (3)$$

As shown in (2) the engine switches to $M = R$ after n_t cycles.

C. Cold Start

Cold starting the engine leads to increased fuel consumption. For that reason a respective penalty was introduced. The first phase of the FTP-75 driving cycle includes cold start and shows the same reference velocity trajectory as the third phase. Therefore coolant temperature and fuel consumption measurements of those two phases can be compared with each other. Based on those measurements it was observed that the coolant temperature increases linearly with time from 30°C to a steady state temperature of 92°C within 300s. At the same time the penalties on BMEP and fuel decrease in a approximately linear way with time. Due to those findings a linear fit has been used to calculate the time dependency of the fuel penalty during warm up.

A mode switch from SI to HCCI requires high engine temperatures. Therefore it is assumed that until steady state temperature is reached a mode switch to HCCI is not possible.

III. DRIVER MODEL

The drivers main responsibility is to follow the reference velocity $e = v_{ref} - v_v$ specified by the driving cycle, using acceleration and brake pedal positions u_a and u_b. The gear u_g has to follow a predetermined gear shift schedule. The clutch command u_c works as link between engine and wheel speed. Fig. 2 shows the four different driver commands and the main parts of the simulation. Since simulation of the FTP-75 cycle requires driving with slipping clutch the driver behavior is divided into four different driver modes denoted as state ε.

The driver mode $\varepsilon = 1$ is responsible for vehicle control at
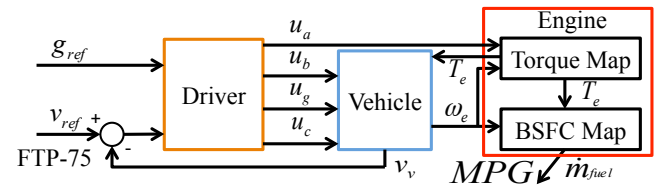

Fig. 2. Block diagram of whole system with connections between driver, vehicle and engine

locked clutch condition. The other three modes are active while the clutch is slipping. This means $\varepsilon = 2$ controls vehicle halt, standstill and launch, $\varepsilon = 3$ upshift and $\varepsilon = 4$ downshift. All the driver modes are explained after the gear controller.

A. Gear Controller

The gear controller initiates the shifts of gear u_g to follow the reference g_{ref}. The up- and downshifts are divided into two sequences and the gear actually up or downshifts in between. Those sequences are used below to time the feed forward controllers.

B. Driver Mode $\varepsilon = 1$, Locked

While $\varepsilon = 1$, the driver mode switch is determined by,

$$\varepsilon(k+1) = \begin{cases} 3 & \sigma(k) = 1 \\ 4 & \sigma(k) = -1 \\ 2 & \omega_e < \omega_{e,min} \wedge \sigma(k) = 0 \\ 1 & \text{else.} \end{cases} \quad (4)$$

A PI controller for the acceleration pedal is being used while Driver Mode 1 is active, together with a PI controller for braking if the acceleration pedal is fully released,

$$u_a = \text{PI}_{a,1}(s) \cdot e \quad (5)$$

$$u_b = \begin{cases} -\text{PI}_{b,1}(s) \cdot e & u_a = 0 \wedge e < 0\frac{m}{s} \\ 0 & \text{else.} \end{cases} \quad (6)$$

C. Driver Mode $\varepsilon = 2$, Unlocked - Halt & Launch

During $\varepsilon = 2$, the clutch l determines the switch,

$$\varepsilon(k+1) = \begin{cases} 1 & l = 1 \\ 2 & l = 0. \end{cases} \quad (7)$$

For low engine speeds the no-kill condition must be fulfilled, i.e. one must avoid engine stall. During $\varepsilon = 2$ u_a keeps ω_e idling. Even though MIMO, the system is diagonally dominant and a SISO-control approach can be used to control engine and vehicle speed separately.

$$u_a = \text{PI}_{a,2}(s) \cdot (\omega_{e,ref} - \omega_e) \quad (8)$$

The pedal positions u_b and u_c are responsible to follow the reference speed using PI controllers. As long as $v_{ref} = 0$ the u_b is set to one to prevent the vehicle speed from chattering. In addition the brake is only active if $v_{ref} < v_v$:

$$u_b = \begin{cases} 1 & v_{ref} = 0 \\ -\text{PI}_{b,2}(s) \cdot e & v_{ref} \neq 0 \wedge e < 0 \\ 0 & \text{else.} \end{cases} \quad (9)$$

For accelerating and decelerating reference speed the clutch controller is used:

$$u_c = \begin{cases} 0 & v_{ref} = 0 \\ \text{PI}_{c,2}(s) \cdot e & v_{ref} \neq 0. \end{cases} \quad (10)$$

After some time, defined by the closed-loop dynamics, the point $\omega_e = \omega_c$ will be reached, the clutch will lock and both driver ε and drivetrain modes δ will change.

D. Driver Mode $\varepsilon = 3$, Unlocked - Upshift

Since time is required to release the acceleration pedal and to open the clutch, the shift is divided into two phases, one before and one after the actual gear shift. Piecewise linear functions are implemented as feedforward strategies for u_a and u_c. The clutch is opened and the throttle released during the first phase. During the second phase two things have to be accomplished: First of all ω_c has to match ω_e in order to lock the clutch and second of all v_v should approach v_{ref} again. The clutch closes piecewise linearly while the controller $\text{PI}_{a,3}(s)$ is used to accomplish this.

E. Driver Mode $\varepsilon = 4$, Unlocked - Downshift

The downshift process is divided into two phases as well. During the first phase the inputs are zero. For the second phase the controllers $\text{PI}_{a,4}$ and $\text{PI}_{b,4}$ are used to control ω_e and v_v respectively. The reference engine speed decreases linearly until ω_{min} is reached. The clutch command u_c increases linearly until it saturates at the constant value.

IV. VEHICLE MODEL

In order to analyze the engine mode switching behavior during a vehicle driving cycle, the reference velocity of the vehicle has to be translated into engine speed and load. This is done using the following vehicle model.

A. Model Components

By using the binary state l the vehicle model distinguishes between locked clutch $l = 1$ as main drivetrain mode and slipping clutch $l = 0$ used for vehicle standstill, launch, up- and downshift. The deciding clutch logic is based on [8]. The clutch slip i_c determines the sign of the clutch torque T_c:

$$i_c = \omega_e - \omega_c \quad (11)$$

For a slipping clutch the absolute value of the clutch torque is given by the clutch pedal command u_c:

$$T_c = \begin{cases} T_e & l = 1 \\ u_c \cdot \text{sign}(i_c) \cdot T_{c,max} & l = 0 \end{cases} \quad (12)$$

The road load T_r, i.e. rolling friction and aerodynamic drag, is defined as shown by [2]. With the exception of very low vehicle velocities at halt and launch the tire slip model presented by [6] was enabled to compute T_t. The Willans approach was reformulated to model the gear box torque T_g as it was shown in [2] to take care of power losses reducing or increasing T_g with respect to the direction of the power flow, with η_g as the efficiency of the gearbox. The gear ratio γ is determined by the driver command u_g.

$$T_g = \gamma \cdot \begin{cases} \eta_g \cdot T_c & T_e \geq 0 \\ \frac{1}{\eta_g} \cdot T_c & T_e < 0 \end{cases} \quad (13)$$

The friction brake T_b was modeled as a first order element similarly to [4].

B. Drivetrain

The current drivetrain mode is represented by δ. $\delta = 1$ means locked, $\delta = 2$ unlocked with enabled and $\delta = 3$ with disabled tire slip. Equation (14) decides about the drivetrain mode for the next time step where v_v is the vehicle velocity and $v_{min,t}$ is the minimum velocity for tire slip.

$$\delta(k+1) = \begin{cases} 1 & l(k) = 1 \\ 2 & l(k) = 0 \wedge v_v(k) \geq v_{min,t} \\ 3 & l(k) = 0 \wedge v_v(k) < v_{min,t} \end{cases} \quad (14)$$

The second drivetrain mode $\delta = 2$ for the unlocked clutch and tire slip is the most general representation of the system. The three state equations (15), (16) and (17) are used to

calculate engine speed ω_e, wheel speed ω_w and vehicle speed v_v, with T_e and T_c as engine and clutch torques respectively.

$$\Theta_e \frac{d}{dt} \omega_e = T_e - T_c \tag{15}$$

$$\left(\Theta_g \gamma^2 + 4\Theta_w\right) \frac{d}{dt} \omega_w = T_g - T_t - T_b \tag{16}$$

$$m_v \cdot r_w \frac{d}{dt} v_v = T_t - T_r \tag{17}$$

Θ_e is the engine inertia. Θ_g and Θ_w are the inertias of gear box and wheels. Linked over the gear ratio γ they result in the total rotational inertia of drivetrain and wheels. The inertia of the vehicle is calculated using r_w as wheel radius and m_v as mass of the vehicle. The torques T_g, T_t, T_b and T_r represent gear box, tire slip, brake and road load, respectively.

For the first drivetrain mode $\delta = 1$ for the locked clutch the algebraic relationship $\omega_w = \frac{\omega_e}{\gamma}$ can be used to simplify equations (15) and (16). The third drivetrain mode $\delta = 3$ for unlocked clutch with disabled tire slip can be derived using the equation $v_v = r_w \cdot \omega_w$ to reduce equations (16) and (17).

Fig. 3 pictures the block diagram of the system for $\delta = 2$. For the other two modes some blocks can simply be merged.
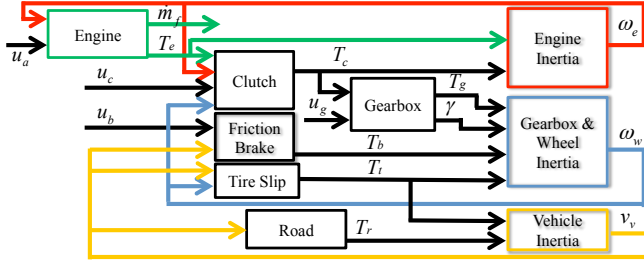

Fig. 3. Block diagram of drivetrain mode 2 simulating slipping clutch with enabled tire slip. The four inputs to the vehicle model are acceleration u_a, brake u_b, clutch u_c pedal positions and the gear u_g.

V. MODEL VALIDATION

Measurements from the FTP-75 driving cycle performed on a vehicle on a chassis dynamometer performed by a human driver are available for the Cadillac CTS equipped with the original 3.6L V6 engine. In order to validate the vehicle model the recorded states are compared for the different driving maneuvers, e.g. regular driving and shift. During regular driving at constant gear, v_{ref} is the only input that varies. As can be seen in Fig. 4 the trajectories for velocity, engine speed and load match very well.

Another, less complex, driving situation is looked at in Fig. 5. A constant increase in reference velocity is shown and as can be seen the model is capable of simulating the behavior of the drivetrain during upshift. A comparison of experimentally measured and simulated vehicle signals shows for both a characteristic decrease in vehicle acceleration between 735-737 s while the clutch is slipping.

Table I compares the FTP-75 fuel mileage results of the simulation with bag emission measurements. The simulation is 15.6% too high. The measured engine torque and speed were
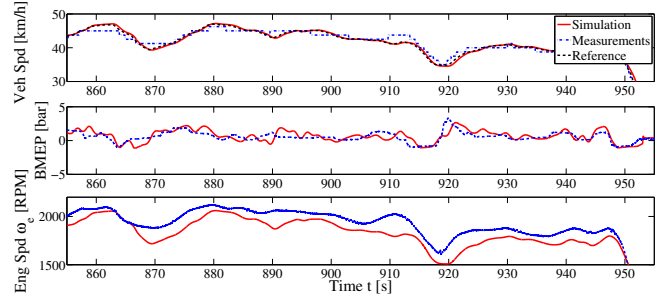

Fig. 4. Comparison of simulated (red solid) and measured (blue dashdot) trajectories for regular driving using driver mode 1. The abrupt changes in the velocity measurement curve are due to quantization. The top plot also includes the reference velocity (black dashed)
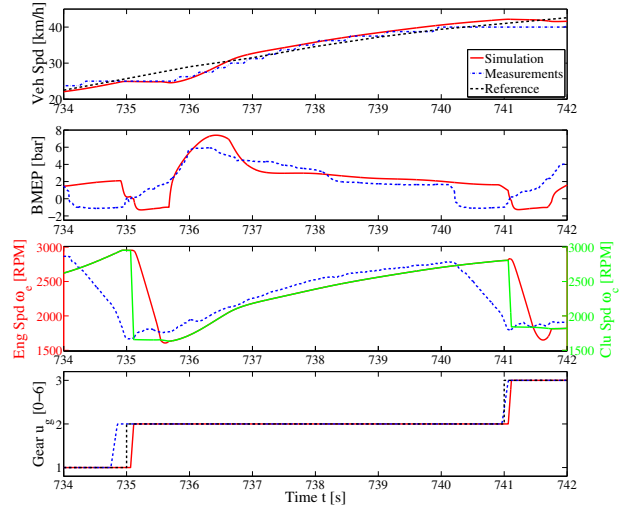

Fig. 5. Comparison of simulated (red solid) and measured (blue dashdot) trajectories for upshift using driver modes 1 and 3. The sharp changes in the velocity measurement curve are due to quantization. The top plot includes the reference velocity (black dashed) while the third plot compares clutch (green solid) and engine speed.

used as inputs to the static BSFC map for comparison. This way the error from using static BSFC maps can estimated. Here, the relative difference to the measurements is very similar, 16.8%. Therefore the difference is most likely caused by the inability of the static maps to predict the fuel consumption during transient engine behavior.

To conclude, the engine speed and load are well predicted by the model during the driving cycle but the use of static BSFC maps, which neglects fast engine cycle dynamics, leads to an overestimated absolute value of the fuel mileage. Note that the influence on fuel economy of the combustion mode transitions, which last for a few cycles, is still captured through the fuel penalty factor d introduced in Sec. II.

TABLE I
SI 3.6L MPG SIMULATION COMPARED TO BAG EMISSIONS

rel. Difference	Phase 1	Phase 2	Phase 3	Total
Simulation	+7.4%	+19.1%	+14.2%	+15.6%
Meas. w/ BSFC map	+10.5%	+20.4%	+13.2%	+16.8%

VI. ANALYSIS OF COMBUSTION MODE TRANSITIONS

After establishing the driver and drivetrain models for the conventional powertrain, the integrated model will now be applied to predict and analyze the fuel consumption of the vehicle with the downsized and two mode engine. The simulation results for the 2.0L I4 engine are analyzed with respect to the stays in the different combustion modes M and according to the regions R. It is assumed that the weight of the 3.6L V6 engine is equal to the weight of the 2.0L I4 due to its stronger engine block for sustaining higher pressure differences together with its additional devices, i.e. turbocharger and variable valve timing. Since vehicle, drivetrain and transmission remain the same during downsizing, the engine torque and speed measurements for the original engine can be used together with the simulation results for an analysis of the 2.0L engine.

A. Instantaneous Transitions

First the mode switches are assumed to be instantaneous, i.e. $n_w = 0$ and $n_t = 0$, which leads to the maximal theoretical use of HCCI for this particular driving cycle. Fig. 6 and Table II show the results of the analysis. Both, simulation and measurements lead to a fraction of time spent in the HCCI region around 25%. This is the maximum possible use of HCCI in the FTP-75 cycle even if mode transitions are assumed to be instantaneous. As can be seen especially for the measurements but confirmed also with the simulation results, a large number of stays are very short. The extremely high fraction of very short stays for the measurements in Fig. 6 can be explained with the noisy torque signal.

The short duration of HCCI stays brings up two important issues that limit the HCCI mode: First, the mode transitions require time, so it does not make sense to switch to HCCI if the stay will probably be shorter than the time required to transition. A second constraint is the penalty on fuel during mode switches: The fuel benefits from an average stay in HCCI are compared to SI. The higher efficiency has to be maintained or be greater even if it accounts for what has to be spent additionally on the transitions to switch the modes.

To account for the first issue the assumption made in section II-B for a transition duration $n_t = 5$ cycles plus $n_w = 1$ cycle can be used as a lower bound. By deleting all the cycles shorter than six the whole distribution shifts six cycles to the left. This leads to a decrease in the total number of stays, for simulation and measurements from 193 to 140 and from 221 to 104 respectively, i.e. the fraction of time spent in HCCI mode will be reduced as well. At the same time the average duration of a stay increases, from 43 to 52 cycles and from 38 to 73 cycles for simulation and measurements respectively. To account for the second issue it is possible to increase the average duration by delaying a switch to HCCI. Up to a certain value excluding shorter stays increases the average duration of a stay more than what must be subtracted by waiting. Therefore, for a given fuel penalty and transition duration, an optimum with respect to fuel consumption between total time spent in HCCI and number of transitions should exist.

This approach is from now on referred to as wait or smoothing strategy and is one possible way to influence the average duration of a stay. Another strategy might involve the use of the rate of change of the engine load at region entry in order to characterize the duration of the stay.
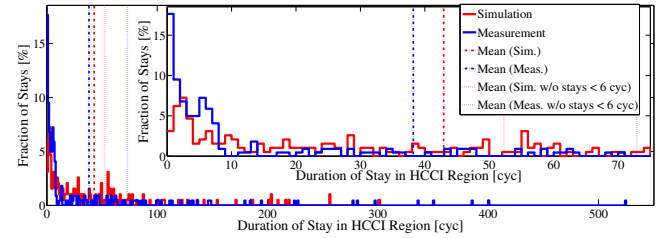

Fig. 6. Distribution of fraction of stays in the HCCI region for different durations for the FTP-75. Simulation (red) and measurements (blue), main plot shows full distribution, insert a zoom in.

TABLE II
HCCI REGION ANALYSIS FOR THE FTP-75

	Simulation	Measurements
Total number of stays	193	221
(w/o Stays < 6 cyc)	140	104
Fraction of time in HCCI region [%]	24.9	24.9
Mean duration of stays [cyc]	43	38
(w/o stays < 6 cyc) [cyc]	52	73

B. Penalized Transitions

Further analysis is now presented for more physical mode transitions into HCCI, including transition penalty and duration as well wait duration, d, n_t and n_w, respectively. As mentioned in Sec. II-B a constant transition duration of $n_t = 5$ cycles is assumed.

The fuel penalty d is varied from 1 to 2, $d = 1$ representing SI fuel consumption during the mode transitions. In Fig. 7 the ratio between HCCI and SI fuel mileage is depicted over fuel penalty and wait duration. As can be seen the influence of transitions can be significant. The black lines represent the contour lines of the SI fuel mileage. HCCI configurations above those lines are more efficient than SI. If no wait mode is enabled a transition penalty $d \geq 1.53 - 1.6$ cancels the benefits of HCCI on fuel consumption for both simulation and measurements. The wait duration n_w is used to minimize BSFC for the variation of the fuel penalty d:

$$n_w^*(d) = \underset{n_w}{\operatorname{argmin}} \ \mathrm{BSFC}(n_w, d) \qquad (18)$$

The optimal wait durations $n_w^*(d)$ are highlighted. For very small penalties, the wait strategy does not increase efficiency. But for $d > 1.15$ delaying of the mode switch is beneficial and the optimum wait duration increases. In Fig. 8 again the ratio of HCCI over SI fuel mileage is plotted for simulation and measurements over the variation of the fuel penalty. The two opposite mode transition strategies are compared. Specifically, no waiting and direct switch to the transition mode and optimal wait duration $n_w^*(d)$.
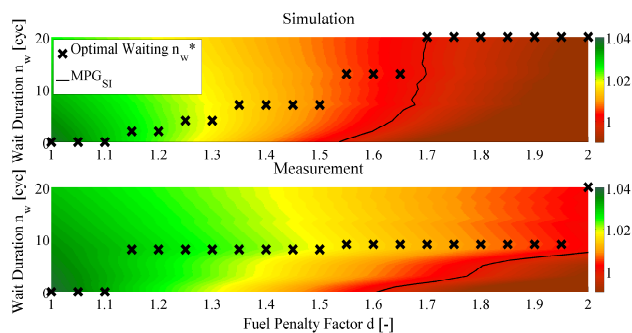
Fig. 7. Plot of the ratio of HCCI over SI fuel mileage in dependence on fuel penalty during transition and duration of waiting. The top plot for the simulation, the bottom plot for the measurements. X mark the fuel optimal wait durations for different penalty factors. On the solid black line HCCI and SI have the same overall efficiency.

The perfect case without penalty and instantaneous mode switch is shown in Fig. 8 on the left side. As can be seen, the gain in fuel mileage lies over 4% compared to SI. An increase in d to 1.25 already cuts the gain of HCCI in half; after an increase to 1.4 only one quarter of the gain in fuel mileage is left. Therefore optimizing the control strategy for mode switches is crucial.

For higher fuel penalties already delaying the mode switch by using the optimal wait duration retains parts of the HCCI benefits, e.g. for the measurements the penalty where only a quarter of the benefits is left is shifted from 1.43 to 1.75.
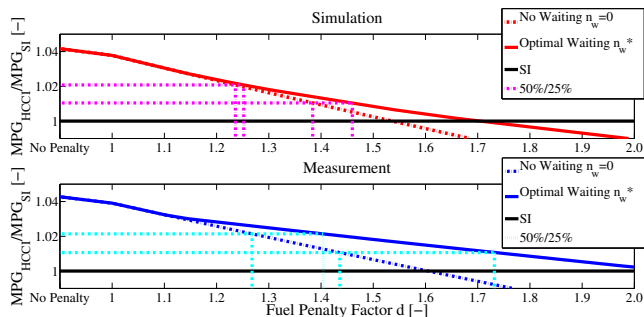

Fig. 8. Ratio of HCCI over SI fuel mileage for simulation (top) and measurements (bottom) over the fuel penalty and instantaneous switch at the left. Two wait strategies are compared: No (dotted) and optimal waiting (solid). Half and fourth of the benefits are highlighted (dotted, thin).

VII. CONCLUSIONS

A dynamic vehicle and driver model, capable of simulating driving cycles, was introduced and subsequently applied for analyzing the influence of combustion mode switches on fuel consumption during the FTP-75 driving cycle. It was found that the increased fuel consumption during transitions between the combustion modes SI and HCCI is able to negate a significant part of the advantages of HCCI. In order to reduce this influence, depending on the penalty on fuel consumption, an optimal number of cycles was calculated by which the combustion mode switch should be delayed. In future work the engine model will be extended to include combustion

mode switches to spark-assisted compression ignition (SACI) and the mode switch analysis will be applied to additional driving cycles such as the HWFET. Also this model will be used to evaluate the fuel economy impact of various mode coordination and transition strategies.

REFERENCES

[1] P. Gorzelic, E. Hellström, L. Jiang, and A. Stefanopoulou. Model-based feedback control for an automated transfer out of SI operation during SI to HCCI transitions in gasoline engines. In *Dynamic Systems and Control Conference*, 2012.

[2] L. Guzzella and A. Sciarretta. *Vehicle Propulsion Systems, Introduction to Modeling and Optimization*. Springer, 2007.

[3] P.-A. Hansson, M. Lindgren, M. Nordin, and O. Pettersson. A methodology for measuring the effects of transient loads on the fuel efficiency of agricultural tractors. *Applied Engineering in Agriculture*, 19:251–257, 2003.

[4] D.H. McMahon, J.K. Hedrick, and S.E. Shladover. Vehicle modelling and control for automated highway systems. In *American Control Conference*, 1990.

[5] E. Ortiz-Soto, D. Assanis, and A. Babajimopoulos. A comprehensive engine to drive-cycle modelling framework for the fuel economy assessment of advanced engine and combustion technologies. *International Journal of Engine Research*, 13:287–304, 2012.

[6] H. Pacejka, E. Bakker, and L. Nyborg. Tyre modelling for use in vehicle dynamics studies. *SAE Technical Paper*, 1987.

[7] M. Roelle, G. Shaver, and J. Gerdes. Tackling the transition: A multi-mode combustion model of SI and HCCI for mode transition control. In *Proceedings of IMECE*, 2004.

[8] The MathWorks, Inc. *Using Simulink and Stateflow in Automotive Applications*. 1998.

[9] H.Y. Tong, W.T. Hung, and C.S. Cheung. On-road motor vehicle emissions and fuel consumption in urban driving conditions. *Journal of the Air & Waste Management Association*, 50:4:543–554, 2011.

[10] X. Yang and G.G. Zhu. SI and HCCI combustion mode transition control of an hcci capable engine. *IEEE Transactions on Control Systems Technology*, PP:1, 2012.

[11] H. Yun, N. Wermuth, and P. Najt. Developement of robust gasoline HCCI idle operation using multiple injection and multiple ignition (MIMI) strategy. In *SAE World Congress & Exhibition*, 2009.

[12] Y. Zhang, H. Xie, and H. Zhao. Investigation of SI-HCCI hybrid combustion and control strategies for combustion mode switching in a four-stroke gasoline engine. *Combustion Science and Technology*, 181:782–799, 2009.

[13] R. Zhen and G.G. Zhu. Modeling and control of an electric variable valve timing system for SI and HCCI combustion mode transition. In *American Control Conference 2011*, 2011.